CHAPTER W19

Surfaces

W19.1 Surface States

It is possible to introduce Tamm surface states by adding an attractive delta function potential of strength U to the step potential introduced in Eq. (19.3):[†]

$$V(z) = -V_0\Theta(-z) - U\delta(z). \tag{W19.1}$$

Note that the units of U are J·m and that of V_0 are joules. The independent variables in the Schrödinger equation can be separated with the substitution

$$\psi(\mathbf{r}) = \phi(z)\exp(i\mathbf{k}_\parallel \cdot \mathbf{r}_\parallel) \tag{W19.2}$$

where a solution can be found with

$$\phi(z) = \begin{cases} \exp(-\kappa z) & \text{if} \quad z > 0, \\ \exp(+qz) & \text{if} \quad z < 0. \end{cases} \tag{W19.3}$$

Here

$$\kappa = \sqrt{k_\parallel^2 - \frac{2mE}{\hbar^2}}, \tag{W19.4a}$$

where $E < 0$ and

$$q = \sqrt{k_\parallel^2 - \frac{2m(E+V_0)}{\hbar^2}}. \tag{W19.4b}$$

The function $\phi(z)$ is continuous at $z = 0$. The discontinuity in the derivative is determined by the strength of the delta function:

$$\sqrt{k_\parallel^2 - \frac{2mE}{\hbar^2}} + \sqrt{k_\parallel^2 - \frac{2m(E+V_0)}{\hbar^2}} = \frac{2mU}{\hbar^2}. \tag{W19.5}$$

The solution to this equation gives the dispersion formula for the surface state band, $E(k_\parallel)$. Note that at $k_\parallel = 0$, E must lie below $-V_0$.

[†] The material on this home page is supplemental to *The Physics and Chemistry of Materials* by Joel I Gersten and Frederick W. Smith. Cross-references to material herein are prefixed by a "W"; cross-references to material in the textbook appear without the "W".

For the Shockley state one may develop a heuristic model to help understand its origin. Consider a semiconductor and look at the states near the top of the valence band at energy E_v. For simplicity's sake the effective mass of the holes will be assumed to be isotropic and the band will be taken to be parabolic. The energy of an *electron* in the valence band is then given by

$$E(k) = E_v - \frac{(\hbar k)^2}{2m_h^*}. \tag{W19.6}$$

One may develop a phenomenological Schrödinger equation based on a spatially dependent mass $m(z)$ with $m(z)$ being the free-electron mass in vacuum and the negative of the hole mass inside, that is,

$$m(z) = \begin{cases} -m_h^* & \text{if} \quad z < 0 \\ +m & \text{if} \quad z > 0. \end{cases} \tag{W19.7}$$

The resulting Schrödinger equation is

$$-\frac{\hbar^2}{2}\nabla \cdot \left[\frac{1}{m(z)}\nabla\phi\right] + E_v\Theta(-z)\phi = E\phi. \tag{W19.8}$$

(The gradient operator is written in this split form so that the probability current perpendicular to the surface may be proven to be continuous.)

As before, look for a solution of the form given by Eqs. (W19.2) and (W19.3). Now

$$q = \sqrt{\frac{2m_h^*}{\hbar^2}(E - E_v) + k_\parallel^2}, \tag{W19.9a}$$

$$\kappa = \sqrt{k_\parallel^2 - \frac{2mE}{\hbar^2}}. \tag{W19.9b}$$

The wavefunction $\phi(z)$ in Eq. (W19.3) is already continuous. The continuity of probability current perpendicular to the surface,

$$-\frac{\hbar}{m_h^*}\mathrm{Im}\left(\phi^*\frac{d\phi}{dz}\right) = \frac{\hbar}{m}\mathrm{Im}\left(\phi^*\frac{d\phi}{dz}\right), \tag{W19.10}$$

which is needed for a valid wavefunction, implies that

$$\frac{q}{m_h^*} = \frac{\kappa}{m}. \tag{W19.11}$$

Thus the condition for the surface-state band is

$$\frac{1}{m_h^*}\sqrt{\frac{2m_h^*}{\hbar^2}(E - E_v) + k_\parallel^2} = \frac{1}{m}\sqrt{k_\parallel^2 - \frac{2mE}{\hbar^2}}. \tag{W19.12}$$

For $k_{\|} = 0$ the surface state lies at an energy above the top of the valence band ($E > -|E_v|$) but below the vacuum level ($E < 0$):

$$E(k_{\|} = 0) = -\frac{|E_v|}{1 + m_h^*/m}. \tag{W19.13}$$

More generally, one often employs a complex band structure in which the bulk energy bands are extended to negative values of k^2. This permits an effective Hamiltonian for the solid to be written which may be solved in conjunction with the Hamiltonian for the electron in vacuum. The procedure of wavefunction matching is similar to what was employed, but the implementation is more computational.

W19.2 Surfactants

Surface-active agents, or *surfactants*, are molecules that can radically alter the surface or interface properties of a system even in small concentrations. The system usually involves the liquid–solid, liquid–liquid, or liquid–gas interface. Sometimes the term *surfactant* is used in reference to adsorbates [e.g., a monolayer of As is used on Si (100) and Ge (100) to aid in Si–Ge heteroepitaxy]. Here, however, the focus is on the liquid–solid interface. The surfactant molecule can consist of a long hydrocarbon chain with an polar unit at one end. In the liquid the hydrocarbon chain must push aside the liquid molecules to make room for the surfactant molecule. This involves reducing the forces responsible for the liquid bonds. In water the surfactant molecule must break apart the hydrogen bonds that exist. Since the hydrocarbon chain has all its valence requirements satisfied by carbon–carbon or carbon–hydrogen bonds, it is fairly inert to chemical or electrical interactions with the liquid. The net result is that the liquid tends to expel the hydrocarbon in order to lower its energy. The hydrocarbon chain is called *hydrophobic*, since it avoids being in water. On the other hand, the polar end can lower its energy by immersing itself in the liquid. There is an electrical attraction between the polar group and the liquid. This end is called *hydrophilic*, due to its affinity for water. In order for the molecule to go into solution, the energy decrease involved in the hydrophilic interaction must be greater than the energy increase due to the hydrophobic interaction. Typical examples of surfactant molecules are $C_{12}H_{25}SO_4{}^-Na^+$ and $C_{12}H_{23}COO^-Na^+$.

The surface or interface provides a region of space where both the hydrophobic and hydrophilic tendencies can be satisfied simultaneously. If the polar group lies in the liquid and the hydrocarbon chemisorbs onto the surface, a doubly low energy can be achieved. The lowest-energy state of the system therefore involves an accumulation of the surfactant molecules at the surface. This means that even in small concentrations the molecules will aggregate at the surface.

The adsorption of the surfactants at the surface or interface lowers the interfacial tension, often significantly. This can radically alter such properties as surface diffusion, chemisorption, and crystal growth. Since the surface atoms are now binding themselves to the surfactant molecules, they have fewer bonding electrons to form the surface bonds, thereby depressing the surface tension.

The surface tension drops monotonically with increasing surfactant concentration until a critical concentration is reached (usually when the surface is completely covered). Beyond that the surface properties no longer change. This curious behavior is traced to an interaction that the surfactant molecules have among themselves. The

surfactant molecules can form a composite unit in solution called a *micelle*. The micelle comes about, for example, by creating a ball of molecules with their hydrocarbon chains directed toward the center of the sphere and the polar groups directed outward into the liquid. Liquid is not present in the interior of the micelle. This also satisfies both the hydrophobic and hydrophilic tendencies of the molecule. Other geometries, involving micellar rods or parallel sheets, are also possible.

To understand why a surfactant molecule would prefer to leave the liquid and adsorb onto a surface, one must compare the energies of the molecule in solution with it being adsorbed on the surface. A crude model for the interaction of the surfactant molecule with the liquid may be obtained by imagining that the polar end is a point dipole that carves out a small spherical cavity around it in the liquid. Let the sphere have a radius equal to a. Denote the strength of the dipole by μ, and the electric permittivity of the liquid by ϵ. The electrostatic potential in all of space is then given by

$$\Phi(r,\theta) = \begin{cases} -E_0 r\cos\theta + \dfrac{\mu\cos\theta}{4\pi\epsilon_0 r^2} & \text{if} \quad r < a, \\ \dfrac{p\cos\theta}{4\pi\epsilon r^2} & \text{if} \quad r > a, \end{cases} \tag{W19.14}$$

where, in order to satisfy the continuity of Φ and the radial component of the electric displacement vector D_r

$$p = \frac{3\mu\epsilon}{\epsilon_0 + 2\epsilon}, \tag{W19.15}$$

$$E_0 = \frac{2\mu}{4\pi\epsilon_0 a^3}\frac{\epsilon - \epsilon_0}{\epsilon_0 + 2\epsilon}. \tag{W19.16}$$

Here E_0 is the electric field in the cavity due to the polarization charges in the liquid. The interaction energy of the dipole with this field, U_s, is called the *solvation energy*:

$$U_s = -\frac{\mu^2}{4\pi\epsilon_0 a^3}\frac{\epsilon - \epsilon_0}{\epsilon_0 + 2\epsilon}. \tag{W19.17}$$

The hydrophobic interaction, U_i, may be estimated by imagining that the hydrocarbon chain carves out a cylindrical cavity with surface area A. This causes a rise in the surface energy given approximately by the product of the surface tension of the liquid and the area

$$U_i = \gamma A. \tag{W19.18}$$

For the molecule to go into solution, the total energy, $U_s + U_i$, must be negative. When chemisorption of the surfactant molecule occurs, there is an additional energy U_c, corresponding to the chemisorption bond. Since $U_c < 0$ it is favorable for the surfactant molecules to go out of solution and adsorb onto the surface.

W19.3 Adsorption

Suppose that a solid is exposed to a monatomic gas at temperature T and pressure P. Atoms will strike the surface and a fraction, s, will stick to it. It is therefore important

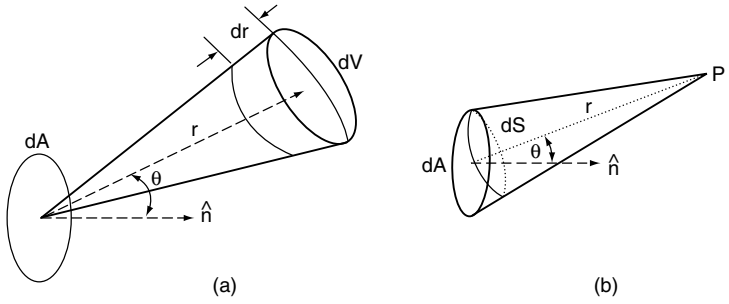

Figure W19.1. An element of area on the surface, dA, and volume element in the gas, dV; particles emanating from a volume element at P strike the element of area dA on the surface.

to determine the impingement flux, F, defined as the number of atoms striking the surface per unit area per unit time. As will be seen, F is determined simply in terms of P, T, and the atomic mass, M.

In Fig. W19.1*a* an element of area dA of the surface is drawn, as well as a volume element dV in the gas a distance r away. The vector joining dA and dV makes an angle θ with the surface normal. The radial extent of dV is dr. The number of atoms in dV is $dN = n\,dV$, where n is the number of atoms per unit volume (number density). For the moment, consider only the subset of atoms moving with a given speed v. These atoms are moving in random directions. Those atoms that are directed approximately at dA will strike it at a time $t = r/v$ later, over a duration lasting $dt = dr/v$. Therefore, the volume element may be expressed as $dV = r^2\,d\Omega v\,dt$, where $d\Omega$ is the solid angle subtended by dV at dA.

The fraction of atoms emanating from dV which strike dA is determined by the solid angle subtended by dA by a typical point in dV, P. Referring to Fig. W19.1*b*, the solid angle is $d\Omega' = dS/r^2$, where dS is the projection of dA onto a plane perpendicular to r, and is given by $dS = dA\cos\theta$. The desired fraction is $df = dA\cos\theta/4\pi r^2$, where the solid angle has been divided by 4π steradians.

The differential flux is

$$dF = \frac{df}{dA}\frac{dN}{dt} = \frac{nv}{4\pi}\cos\theta\,d\Omega. \tag{W19.19}$$

The net flux is obtained by integrating dF over a hemisphere (using $d\Omega' = 2\pi\sin\theta\,d\theta$, where $0 \le \theta \le \pi/2$), that is,

$$F = \frac{n\langle v\rangle}{4}. \tag{W19.20}$$

Here there is finally an average over all speeds.

The kinetic theory of gases provides a means for computing $\langle v\rangle$:

$$\langle v\rangle = \frac{\int d^3v\,v\exp[-\beta(mv^2/2)]}{\int d^3v\exp[-\beta(mv^2/2)]} = \sqrt{\frac{8}{\pi\beta m}}; \tag{W19.21}$$

here $\beta = 1/k_B T$. Finally, employing the ideal gas law, $P = nk_B T$, the desired expression for the impingement flux is obtained:

$$F = \frac{P}{\sqrt{2\pi M k_B T}}. \tag{W19.22}$$

The rate of deposition of adsorbed atoms per unit area, dN_a/dt, is determined by multiplying the impingement flux by the sticking probability, s. The quantity s is the fraction that stick "forever" (or for at least several vibrational periods). Thus

$$\frac{dN_a}{dt} = \frac{sP}{\sqrt{2\pi M k_B T}}. \tag{W19.23}$$

The sticking probability or coefficient can be a complicated function of the surface conditions and the adsorbed atom areal number density, N_a. Often, this areal density is expressed as the coverage, θ, which is the fraction of a monolayer that is adsorbed (i.e., $\theta = N_a/N_{am}$). For example, at low temperatures, s for N_2 on W(110) first rises and then falls as θ increases. For N_2 on W(100), however, s decreases monotonically with increasing coverage. Different faces of the same crystal can have different values of s. For example, for W(100) $s = 0.6$ at $\theta = 0$, whereas $s = 0.4$ for W(411) and $s = 0.08$ for W(111). The existence of steps on the surface often increases the value of s over what it would be for a smooth surface. For example, s for N_2 adsorbing on Pt (110) increases from 0.3 for a smooth surface to 1.0 for a step density of 8×10^8 m^{-1}. This trend is to be expected since steps generally possess dangling bonds which enhance the degree of chemical reactivity.

The impingement flux is rather high at normal atmospheric pressure. For example, for air at room temperature the flux is 3×10^{27} atoms/m^2·s. Taking $s \approx 1$, one sees that a monolayer ($N_a \approx 10^{19}$ m^{-2}) will be deposited on the surface in about 10^{-8} s. To study a clean surface, ultrahigh-vacuum conditions must be maintained, with pressures as low as 10^{-12} torr, 760 torr being 1 atmosphere of pressure. This often requires preparing the sample under ultrahigh-vacuum conditions, as well. The unit of exposure of a surface to a gas is called the *langmuir*; 1 langmuir corresponds to an exposure of 10^{-6} torr·s.

Once the atom strikes the surface and sticks, at least temporarily, it will migrate from place to place by a series of thermally activated jumps. Most of the time, however, will be spent at adsorption sites. These sites correspond to the minima of the potential energy surface. Typical places for these sites are illustrated in Fig. W19.2, which shows the on-top site, T; the bridge site, B; and the centered site, C, for two crystal faces. More complicated sites can exist for other crystal faces. Steps, kinks, and defect sites are also common adsorption sites.

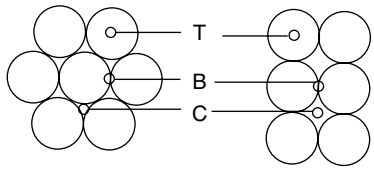

Figure W19.2. The top site, T, the bridge site, B, and the centered site, C for two crystal faces. The left face could be FCC (111) or HCP (0001). The right face could be FCC (100) or BCC (100).

W19.4 Desorption

Desorption is the inverse process to adsorption. Atoms bound in the potential well of the surface vibrate at a characteristic vibrational frequency determined by the atomic mass and the curvature at the bottom of the well. In addition, the atoms interact with the bath of thermal phonons presented by the solid. This causes the energy of the adsorbed atom to fluctuate in time. When the energy fluctuates by an amount sufficient to overcome the binding energy, the atom can dissociate from the surface and be desorbed. The vaporization process is described in terms of desorption in Section 6.3 of the textbook.

A reasonable estimate for the rate of atoms per unit area that desorb may be obtained from the expression

$$\frac{dN_d}{dt} = N_a f \exp\left(-\frac{E_c}{k_B T_s}\right). \tag{W19.24}$$

Here N_a is the number of atoms adsorbed per unit area, f the vibrational frequency of the atoms, and T_s the surface temperature. The probability of the atom achieving the required energy E_c is given by the Boltzmann factor. The factor f represents the "attempt" frequency. In using this expression the situation depicted in Fig. 19.15*a* applies. For the case of a second physisorption well, as in Fig. 19.15*b*, E_p should be used in place of E_c and the density of physisorbed atoms, N_p, should be used rather than the density of chemisorbed atoms, N_a.

In thermal equilibrium the surface and gas temperatures are equal, $T_s = T$, and the adsorption rate equals the desorption rate. Under these conditions it can be shown that

$$N_a(T) = \frac{sP}{f\sqrt{2\pi M k_B T}} \exp\left(\frac{E_c}{k_B T}\right). \tag{W19.25}$$

Thus the number density of adsorbed atoms is proportional to the pressure of adsorbate atoms in the gas.

Now proceed to look at the Langmuir model for adsorption. In this model one regards the surface as having a density of adsorption sites, N_s (denoted by N_{am} in Section W19.3). The sticking probability is modified as these sites are filled with adsorbate atoms. When all the sites are filled, the adsorption process comes to a halt. This model is not general. It applies to a restricted set of adsorption processes, usually corresponding to a strong chemisorption bond formed between the solid and the adsorbate.

Let θ denote the fraction of sites that are occupied, that is,

$$\theta = \frac{N_a}{N_s}. \tag{W19.26}$$

In place of the previous sticking probability, s, one now has $s(1-\theta)$. Thus, equating the adsorption rate to the desorption rate yields

$$\frac{sP(1-\theta)}{\sqrt{2\pi M k_B T}} = N_s \theta f \exp\left(-\frac{E_c}{k_B T}\right). \tag{W19.27}$$

Solving for θ gives the *Langmuir adsorption isotherm*,

$$\theta(P, T) = \frac{aP}{1 + aP}, \tag{W19.28}$$

where

$$a(T) = \frac{s}{N_s f \sqrt{2\pi M k_B T}} \exp\left(\frac{E_c}{k_B T}\right). \tag{W19.29}$$

The formulas above show that the surface coverage saturates to $\theta = 1$ at high gas pressures.

More sophisticated models have been constructed to describe the situation where multilayer adsorption and desorption can occur.

W19.5 Surface Diffusion

The normal state of affairs for adsorbed atoms is for them to move around on the surface at finite temperatures. This is in contrast to the bulk solid, where diffusion occurs via vacancies or interstitials present under equilibrium conditions. Surface diffusion proceeds by a series of thermally activated jumps. In general, no atoms of the substrate have to be "pushed" out of the way to achieve this jump. In this sense it is different from the bulk solid.

Consider a surface that has rectangular symmetry. The diffusion equation for the motion of the adsorbed atoms will be derived. Let the probability for finding an atom in the surface net cell (x, y) at time t be denoted by $F(x, y, t)$. The probability is just the concentration of adsorbed atoms divided by the concentration of available sites, $F = N_a/N_s$. Let p_x be the probability that the atom makes a jump of size d_x in the positive x-direction in a time τ. For the y direction the analogous jump probability involves d_y. Attention will be restricted to the case where there is surface reflection symmetry, so p_x is also the probability for a jump to the point $x - d_x$. At time $t + \tau$ the probability becomes

$$\begin{aligned} F(x, y, t + \tau) = (1 - 2p_x - 2p_y)F(x, y, t) + p_x[F(x + d_x, y, t) + F(x - d_x, y, t)] \\ + p_y[F(x, y + d_y, t) + F(x, y - d_y, t)]. \end{aligned} \tag{W19.30}$$

The first term on the right-hand side represents the probability for the atom originally at (x, y) to have remained on the site. The second and third terms together give the probability that neighboring atoms hop onto the site. Expanding both sides in powers of τ, d_x, and d_y, and retaining lowest-order nonvanishing terms, leads to the diffusion equation

$$\frac{\partial F}{\partial t} = D_x \frac{\partial^2 F}{\partial x^2} + D_y \frac{\partial^2 F}{\partial y^2}, \tag{W19.31}$$

where the diffusion coefficients are

$$D_x = \frac{p_x d_x^2}{\tau}, \qquad D_x = \frac{p_y d_y^2}{\tau}. \tag{W19.32}$$

In the case where there is square symmetry, the two diffusion coefficients become equal to each other and may be replaced by a common symbol, D.

Instead of talking about probabilities, it is more useful to talk about surface concentration, which will now be denoted by C (i.e., $C = N_a = N_s F$). Equation (W19.31) is obeyed by C, since one need only multiply through by N_s. In the derivation above it was assumed that the hopping probabilities are independent of whether or not the site to which it hops is occupied. This is clearly a limitation. It may be remedied by allowing the diffusion constants themselves to be functions of the particle concentration. One may introduce a particle current per unit length, $\mathbf{J}$, defined as the number of adsorbed atoms hopping across a line of unit length per unit time. Suppose, for example, that the surface is horizontal and a line is drawn from south to north. If there is a higher concentration to the east of the line than to the west, there will be a larger number of atoms jumping to the west than to the east. Thus the current will be proportional to the gradient of the probability. Using arguments similar to those used before leads to

$$\mathbf{J} = -\mathbf{D} \cdot \nabla C. \tag{W19.33}$$

Here a diffusion matrix, $\mathbf{D}$, has been introduced and the possibility of having off-diagonal terms must be allowed for.

The continuity equation that governs the flow of particles on the surface is

$$\nabla \cdot \mathbf{J} + \frac{\partial C}{\partial t} = \left(\frac{dC}{dt}\right)_{\text{adsorb}} - \left(\frac{dC}{dt}\right)_{\text{desorb}}. \tag{W19.34}$$

The terms on the right-hand side correspond to the increase or decrease in concentration due to adsorption and desorption, respectively. One thereby obtains the generalized diffusion equation:

$$-\nabla \cdot (\mathbf{D} \cdot \nabla C) + \frac{\partial C}{\partial t} = \left(\frac{dC}{dt}\right)_{\text{adsorb}} - \left(\frac{dC}{dt}\right)_{\text{desorb}}. \tag{W19.35}$$

For pure surface diffusion, the right-hand side of this equation would be zero.

In the diffusion process the probability for making a hop depends on the surface temperature, T_s, and the surface barrier height, E_b;

$$p_x(T_s) = \tau f \exp\left(-\frac{E_b}{k_B T_s}\right). \tag{W19.36}$$

Here f is the attempt frequency, which is essentially the vibrational frequency of the adatom parallel to the surface. In this formula, both the attempt frequency and the barrier height may be different for the x and y directions. For simplicity's sake, attention will henceforth be restricted to the case of square symmetry. Since the hopping probabilities exhibit Arrhenius-type behavior, the diffusion coefficient will also exhibit such behavior. The higher the temperature, the greater will be the rate of surface diffusion.

The solution to the homogeneous diffusion equation, ignoring adsorption and desorption, in two dimensions subject to the initial condition is $C(\mathbf{r}, t = 0) = C_0\delta(\mathbf{r})$ is

$$C(r, t) = \frac{C_0}{4\pi Dt} \exp\left(-\frac{r^2}{4Dt}\right). \tag{W19.37}$$

This may be verified for $t > 0$ by insertion of this formula into the diffusion equation. [Note that $C(r, t)$ and C_0 do not have the same dimensions.] As $t \to 0$ the spatial extent of C becomes narrower and the size of C increases without bound, but the integral over area remains fixed at the value C_0, consistent with the initial condition. This concentration function may be used to compute the mean-square displacement, that is,

$$\langle r^2 \rangle = \frac{\int C(r, t) r^2 dA}{C_0} = 4Dt. \tag{W19.38}$$

The mean-square displacement that a particle travels from its starting point grows as the square root of time for diffusive motion. This is to be contrasted with the case of ballistic motion, where the distance covered grows linearly with t. The presence of surface defects may play an important role in surface diffusion because they often offer paths of high mobility for the diffusing atoms. They may also trap diffusing atoms (e.g., dislocations can pull surface atoms into the bulk or ledges may trap atoms).

One way of observing surface diffusion is by means of the field-ion microscope. Using the atomic-scale resolution capabilities of the microscope permits one to follow the path of a single atom. Usually, the temperature of the tip of the microscope is raised, and the temperature is maintained for some time and then cooled. At elevated temperatures the atom has a chance to hop to an adjacent site. In this way the random walk associated with diffusive motion may be studied. The diffusion coefficient may be extracted from Eq. (19.38) and studied as a function of temperature. From the Arrhenius behavior of D the barrier height E_b may be determined.

W19.6 Catalysis

Surfaces of solids may be used to promote or accelerate particular chemical reactions selectively. Such a catalytic process generally involves the following steps: adsorption of molecules onto the surface; dissociation of the molecules into smaller components (including possibly atoms); diffusion of the components on the surface; reaction of the components to form product molecules; and finally, desorption of the product from the solid. Each of these steps generally involves potential barriers that need to be surmounted, so there are a number of physical parameters governing the overall reaction rate.

Consider, for example, the Haber process for the synthesis of ammonia. Historically, this process has proven to be extremely important because of the role of ammonia as a primary starting material in the manufacture of fertilizers and explosives. The process is illustrated in Fig. W19.3.

The catalyst used is iron. When nitrogen molecules adsorb on iron, the dissociation energy for N_2 is lowered. This is because some of the orbitals that were previously involved in the N–N bond now hybridize with the Fe $3d$ orbitals and serve as the basis for establishing the N_2–Fe bond. At elevated surface temperatures ($\approx 400^\circ$C) the

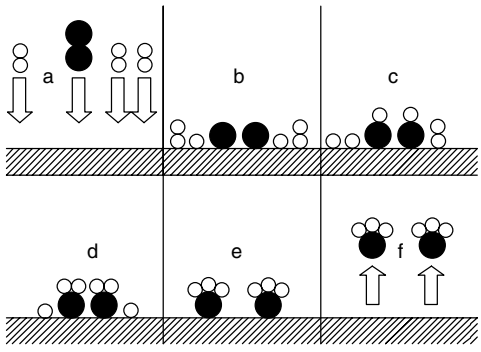

Figure W19.3. Six stages in the Haber process: nitrogen (dark circles) and hydrogen (light circles) combine to form ammonia on iron.

probability for N_2 dissociation increases. The net result is that individual N atoms are bound to the iron and are able to hop from site to site as a result of thermal activation. Hydrogen undergoes a similar dissociation process (i.e., $H_2 \rightarrow H + H$). When a free H and N combine, there is a probability for reacting to form the NH radical, which is still adsorbed. Further hydrogenation results in the formation of NH_2 and ultimately, the saturated NH_3 molecule. Whereas the NH and NH_2 radicals are chemically active, and hence remain chemisorbed to the Fe, the NH_3 is only physisorbed. It is easy for it to desorb. The net result is that Fe has served as the catalyst for the reaction $N_2 + 3H_2 \rightarrow 2NH_3$. Although a number of metals can be used to dissociate N_2 and H_2, Fe is optimal in that it does not attach itself so strongly to N and H so as to prevent their further reacting with each other to reach the desired product, NH_3. What matters is the net turnover rate — how rapidly the overall reaction can be made to proceed per unit area of catalyst.

It is found that some faces of Fe are more catalytically active than others. The Fe (111) and (211) faces are the most active faces, while the (100), (110), and (210) are less active. It is believed that the (111) and (211) faces are special in that they expose an iron ion that is only coordinated to seven other iron atoms (called the C_7 site). It is also found that potassium atoms enhance the sticking coefficient for gas molecules and therefore help promote the catalytic reaction. This is attributed to the lowering of the work function of the surface, which makes it easier for Fe 3*d* orbitals to penetrate into the vacuum so they could form chemical bonds with the adsorbed nitrogen and hydrogen species.

Another example of catalysis is provided by the catalytic convertor used in the automobile industry. Here the problem is to remove carbon monoxide (CO) and nitric oxide (NO) from the exhaust fumes of the internal combustion engine. The catalyst of choice consists of particles of platinum (Pt) and rhodium (Rh) on a (relatively inexpensive) supporting material. An actual catalyst consists of small particles supported on oxide powders. The CO molecule adsorbs on the metal. Some oxygen is present. The O_2 molecules dissociatively adsorb (i.e., $O_2 \rightarrow 2O_{ad}$). Similarly, NO dissociatively adsorbs (i.e., $NO \rightarrow N_{ad} + O_{ad}$). Free N and O atoms diffuse across the surface. When an O atom encounters the CO molecule, the reaction $CO + O \rightarrow CO_2$ is possible. Since the valency requirements of this molecule are fully satisfied, it readily desorbs from the catalyst. The adsorbed N atoms can react similarly to form nitrogen molecules ($N + N \rightarrow N_2$), which also readily desorb.

The morphology of the surface often plays a crucial role in its efficiency as a catalyst. Various crystallographic faces of a given material often have catalytic activities that can vary by orders of magnitude. These large variations reflect the underlying exponential dependence of hopping probability on barrier height. Step sites and other defects often provide locales that favor one or more of the processes needed to transform reactants to products. This is presumably related to the presence of dangling bonds that can be utilized in forming surface-chemical intermediates. Catalysts are frequently used in the form of powders, to maximize the amount of available surface area per unit mass. In some cases coadsorbates are introduced because they provide beneficial surface structures, such as islands, which can play a role similar to that of steps.

W19.7 Friction

The average power generated per unit area by kinetic friction is given by $\mu_k N v/A_a$. This causes an average temperature rise ΔT of the interface. The actual temperature rise will depend on the thermal conductivities κ of the solids and characteristic geometric lengths. One may write the formula as

$$\Delta T = \frac{\mu_k N v}{A_a} \frac{1}{\kappa_1/l_1 + \kappa_2/l_2} = \mu_k P v \frac{1}{\kappa_1/l_1 + \kappa_2/l_2}. \tag{W19.39}$$

where P is the pressure. The lengths l_1 and l_2 correspond to the characteristic distances over which the change ΔT occurs. However, since the actual contact area is much smaller than the apparent contact area, there will be points where the temperature rise is considerably higher. There the temperature rise, to what is called the *flash temperature*, will be given by

$$\Delta T' = \frac{\mu_k N v}{A_t} \frac{1}{\kappa_1/l_1 + \kappa_2/l_2}. \tag{W19.40}$$

This may be a serious problem in ceramics, which generally have low values of κ. The high temperatures produce thermal stresses that lead to brittle fracture. This may be eliminated by depositing a good thermally conducting layer, such as Ag, which serves to dissipate the frictional heat.

A possible explanation for the velocity dependence of μ_k, noted above, is due to the melting of surface asperities. When v becomes sufficiently large, $\Delta T'$ given by Eq. (W19.40) may be large enough to melt the surface asperities.

An interesting case arises if two atomically flat surfaces with different lattice spacings are brought into contact and slide past each other. If the ratio of the lattice spacings is an irrational number, the lattices are said to be *incommensurate*. In that case simulations show that one surface may slowly slide relative to the other without the need to change the number of bonds between them. Furthermore, the energy released by forming a new bond may be resonantly transferred to open a nearby existing bond. There is no static friction predicted in such a case, only viscous friction.

One interesting result of nanotribology is that the kinetic friction force is actually velocity dependent. The force is proportional to the relative velocity at the true contact points. Of course, this velocity may be quite different than the macroscopic velocity due to the local deformations that occur. The kinetic friction force, on a microscopic

level, is actually a viscouslike friction force. The characteristic relaxation time is given by the sliptime.

Lubrication involves attempting to control friction and wear by interposing a third material between the two contacting surfaces. Commonly used solid-state lubricants include the layered materials graphite and MoS_2. Here lubrication is achieved by having weakly bound layers slough off the crystals as shear stress is applied. Liquid lubricants include such organic compounds as paraffins, diethyl phosphonate, chlorinated fatty acids, and diphenyl disulfide. Spherical molecules, such as fullerene, or cylindrical molecules such as carbon nanotubes, behave in much the same way as ball bearings in reducing friction. Lubricants can also carry heat away from flash points or can serve to equalize stress on asperities.

Molecular-dynamics (MD) simulations are often used in conjunction with nanotribology experiments to obtain a more complete understanding of the physics of friction. An example involves the jump-to-contact instability, in which atoms from a surface (such as Au) will be attracted toward an approaching tip of a solid (such as Ni) when the separation is less than 1 nm. At a separation of 0.4 nm, the two metals will actually come into contact by means of this instability.

In another example it was recently found that the amount of slip at a liquid–solid interface is a nonlinear function of the shear rate, $\dot{\gamma}$. If Δv is the relative velocity of the fluid and solid at the interface, Navier had postulated that $\Delta v = L_s \dot{\gamma}$, with L_s being a slip length characteristic of the solid and liquid. The MD simulations[†] show that $L_s = L_s^0(1 - \dot{\gamma}/\dot{\gamma}_c)^{-1/2}$.

The interplay between triboelectricity and friction is not yet completely understood, although there is evidence that the sudden stick-slip motion does produce electrification. When two different materials are brought into contact, a charge transfer will occur to equalize the chemical potential for the electrons. The resulting difference in potential is called the *contact potential*. If the materials are slowly separated from each other the charge transfer is reversed and no electrification occurs. However, for sudden separation, as occurs in a slip, there is incomplete reverse charge transfer and the materials become electrified. It is possible that this accounts for the picosecond bursts of light seen at the moving meniscus of the Hg–glass interface[‡].

Appendix W19A: Construction of the Surface Net

Let $\{\mathbf{R}\}$ be a set of lattice vectors and $\{\mathbf{G}\}$ the corresponding set of reciprocal lattice vectors for a Bravais lattice. The lattice vectors are expressed in terms of the primitive lattice vectors $\{\mathbf{u}_i\}$ $(i = 1, 2, 3)$ by

$$\mathbf{R} = n_1\mathbf{u}_1 + n_2\mathbf{u}_2 + n_3\mathbf{u}_3, \tag{W19A.1}$$

where $\{n_1, n_2, n_3\}$ are a set of integers. Similarly, the reciprocal lattice vectors may be expanded in terms of the basis set $\{\mathbf{g}_j\}$ by

$$\mathbf{G} = j_1\mathbf{g}_1 + j_2\mathbf{g}_2 + j_3\mathbf{g}_3, \tag{W19A.2}$$

[†] P. A. Thomson and S. M. Troian, *Nature*, **389**, 360 (1997).
[‡] R. Budakian et al, *Nature*, **391**, 266 (1998).

where $\{j_1, j_2, j_3\}$ are also a set of integers. The primitive and basis vectors obey the relations

$$\mathbf{u}_i \cdot \mathbf{g}_j = 2\pi\delta_{ij}. \tag{W19A.3}$$

Select an atom at point **O** in the interior of the solid as the origin. Let the surface plane be perpendicular to a particular vector **G** and a distance h from **O**. If the displacement vector **r** from **O** to a point on the surface plane is projected along **G**, the magnitude of this projection is constant. Thus the plane is described by the equation

$$\mathbf{r} \cdot \hat{G} = h \tag{W19A.4}$$

where $\hat{G}$ is a unit vector. This is illustrated in Fig. W19A.1.

Inserting a lattice vector for **r** leads to the formula

$$2\pi(j_1 n_1 + j_2 n_2 + j_3 n_3) = hG. \tag{W19A.5}$$

This equation may be used to eliminate one of the numbers n_1, n_2, or n_3. Which can be eliminated depends on the numbers j_1, j_2, and j_3. If j_1 is nonzero, n_1 may be eliminated and

$$\mathbf{R} = \frac{\mathbf{u}_1}{j_1}\left(\frac{h}{2\pi}G - n_2 j_2 - n_3 j_3\right) + n_2\mathbf{u}_2 + n_3\mathbf{u}_3 \tag{W19A.6}$$

If j_1 is zero, either n_2 can be eliminated (assuming that j_2 is nonzero) or n_3 can be eliminated (assuming that j_3 is nonzero), with analogous formulas for **R** following accordingly. In the following it will be assumed that j_1 is nonzero.

The atoms of the ideal surface plane lie on a regular two-dimensional lattice called the *surface net*. To study this net more closely, project the vector **r** onto the surface lattice plane. Referring to Fig. W19A.2 shows that for a general vector **r** the projected vector is

$$\mathbf{r}' = \mathbf{r} - \mathbf{r} \cdot \hat{G}\hat{G} = \hat{G} \times (\mathbf{r} \times \hat{G}). \tag{W19A.7}$$

Thus a set of projected primitive lattice vectors $\{\mathbf{u}_\mathbf{i}'\}$ can be constructed:

$$\mathbf{u}_1' = \hat{G} \times (\mathbf{u}_1 \times \hat{G}), \tag{W19A.8a}$$

$$\mathbf{u}_2' = \hat{G} \times (\mathbf{u}_2 \times \hat{G}), \tag{W19A.8b}$$

$$\mathbf{u}_3' = \hat{G} \times (\mathbf{u}_3 \times \hat{G}). \tag{W19A.8c}$$

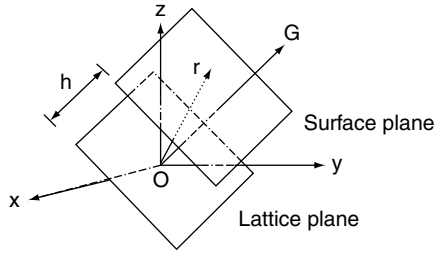

Figure W19A.1. Ideal surface plane defined in terms of the direction of the reciprocal lattice vector, **G**, and h, the distance of an atom at **O**.

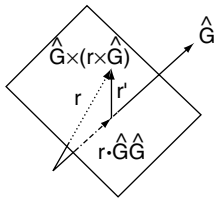

Figure W19A.2. Projecting a vector **r** onto the lattice plane defined by vector **G**.

The projected lattice vector is therefore

$$\mathbf{R}'_{mn} = \frac{h\mathbf{u}'_1}{2\pi j_1} G + n_2\mathbf{v}_2 + n_3\mathbf{v}_3, \tag{W19A.9}$$

where $\mathbf{v}_2$ and $\mathbf{v}_3$ are the primitive surface net vectors, defined by

$$\mathbf{v}_2 = \mathbf{u}'_2 - \frac{j_2}{j_1}\mathbf{u}'_1, \tag{W19A.10a}$$

$$\mathbf{v}_3 = \mathbf{u}'_3 - \frac{j_3}{j_1}\mathbf{u}'_1. \tag{W19A.10b}$$

Note that the projected vector $\mathbf{R}'_{mn}$ is defined by only two subscripts, m and n. The angle between the primitive surface net vectors is determined by the formula

$$\cos\theta = \frac{\mathbf{v}_2 \cdot \mathbf{v}_3}{v_2 v_3}. \tag{W19A.11}$$

(It is convenient to relabel the net vectors so that v_1 and v_2 define the surface net. This is accomplished by making the cyclic permutation $3 \to 2 \to 1 \to 3$.)

In many cases the surface net that results from cutting the lattice by a surface plane is easy to visualize, so one might argue that the mathematical machinery above is superfluous. However, when attempting to automate the procedure, the analytic approach has decided advantages. After all, a computer is not adept at visualization.

Example. Suppose that a simple cubic crystal is sliced by a plane perpendicular to the [111] direction. Take this plane to pass through an atom at the origin. In this case, $j_1, j_2, j_3 = (1, 1, 1)$ and $h = 0$. Thus

$$\hat{G} = \frac{\hat{i} + \hat{j} + \hat{k}}{\sqrt{3}}. \tag{W19A.12}$$

The projected primitive lattice vectors are

$$\mathbf{u}'_1 = \frac{a}{3}(2\hat{i} - \hat{j} - \hat{k}), \tag{W19A.13a}$$

$$\mathbf{u}'_2 = \frac{a}{3}(-\hat{i} + 2\hat{j} - \hat{k}), \tag{W19A.13b}$$

$$\mathbf{u}'_3 = \frac{a}{3}(-\hat{i} - \hat{j} + 2\hat{k}). \tag{W19A.13c}$$

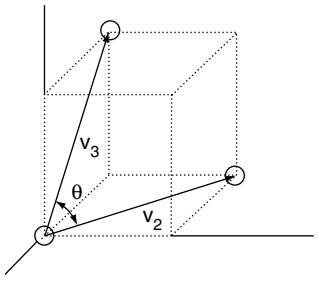

Figure W19A.3. Simple cubic lattice being sliced by a (111) plane passing through the origin.

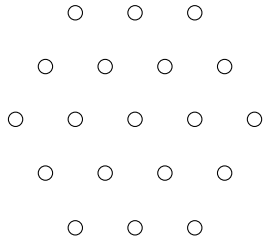

Figure W19A.4. The (111) surface of a simple cubic crystal.

The surface net vectors are

$$\mathbf{v}_2 = a(-\hat{i} + \hat{j}), \tag{W19A.14a}$$

$$\mathbf{v}_3 = a(-\hat{i} + \hat{k}). \tag{W19A.14b}$$

The surface-projected lattice vector is

$$\mathbf{R}'_{mn} = ma(-\hat{i} + \hat{j}) + na(-\hat{i} + \hat{k}). \tag{W19A.15}$$

Figure W19A.3 shows three of the atoms that lie in the surface plane. Figure W19A.4 depicts the layout of the corresponding surface net. It must be emphasized that these two-dimensional nets are the analogs of the Bravais lattices in three dimensions. Just as the lattice in three dimensions may be endowed with a basis of atoms, the same is true in two dimensions.

Applying the formalism above allows one to obtain a precise picture of the surface that results by taking an arbitrary slice through any crystalline structure.

Appendix W19B: Fowler–Nordheim Formula

In this appendix the Fowler–Nordheim formula for the current density produced in field emission is derived. An electric field E_0 is applied normal to a flat metal surface. The potential energy experienced by the electrons is given by

$$V(z) = \begin{cases} 0 & \text{if} \quad z < 0, \\ V_0 - Fz & \text{if} \quad z > 0, \end{cases} \tag{W19B.1}$$

where $F = eE_0$, as illustrated in Fig. 19.11. The Schrödinger equation governing the tunneling process is

$$-\frac{\hbar^2}{2m}\nabla^2\psi(\mathbf{r}) + V(\mathbf{r})\psi(\mathbf{r}) = E\psi(\mathbf{r}). \tag{W19B.2}$$

The transverse motion is decoupled by writing $\psi(\mathbf{r}) = \phi(z)\exp(i\mathbf{k}_\parallel \cdot \mathbf{R})$. In the region $z < 0$ the Schrödinger equation becomes

$$\left(\frac{\partial^2}{\partial z^2} + k_z^2\right)\phi(z) = 0, \tag{W19B.3}$$

where

$$k_z = \sqrt{\frac{2mE}{\hbar^2} - k_\parallel^2}. \tag{W19B.4}$$

The solution of Eq. (W19B.3) is given by

$$\phi(z) = e^{ik_z z} + re^{-ik_z z}, \tag{W19B.5}$$

with r being interpreted as a reflection amplitude.

For $z > 0$ the Schrödinger equation is

$$-\frac{\hbar^2}{2m}\frac{d^2\phi}{dz^2} + (V_0 - Fz)\phi = \frac{\hbar^2 k_z^2}{2m}\phi. \tag{W19B.6}$$

With the substitution

$$u = \left(\frac{2m}{\hbar^2 F^2}\right)^{1/3}\left(V_0 - Fz - \frac{\hbar^2 k_z^2}{2m}\right), \tag{W19B.7}$$

the Schrödinger equation becomes Airy's differential equation:

$$\frac{d^2\phi}{du^2} - u\phi = 0. \tag{W19B.8}$$

The solution may be expressed as a linear combination of the two Airy functions. The coefficients are chosen so that for large x, ϕ represents a wave traveling to the right. Asymptotic expansions of the Airy functions are presented in Table W19B.1. Thus

$$\phi(u) = N[Bi(u) + iAi(u)], \tag{W19B.9}$$

where N is a normalization constant. The current density carried by this wave is given by

$$J_z = \frac{e\hbar}{m}\mathrm{Im}\left(\phi^*\frac{d\phi}{dx}\right) = \frac{e\hbar|N|^2}{m\pi}\left(\frac{2m}{\hbar^2 F^2}\right)^{1/3}F. \tag{W19B.10}$$

TABLE W19B.1 Asymptotic Expansion of the Airy Functions[a]

$Ai(u) \to \frac{1}{2\sqrt{\pi}u^{1/4}}e^{-\zeta}$,	$Ai'(u) \to -\frac{1}{2\sqrt{\pi}}u^{1/4}e^{-\zeta}$
$Bi(u) \to \frac{1}{\sqrt{\pi}u^{1/4}}e^{\zeta}$,	$Bi'(u) \to \frac{1}{\sqrt{\pi}}u^{1/4}e^{\zeta}$
$Ai(-u) \to \frac{1}{\sqrt{\pi}u^{1/4}}\sin\left(\zeta+\frac{\pi}{4}\right)$,	$Ai'(-u) \to -\frac{1}{\sqrt{\pi}}u^{1/4}\cos\left(\zeta+\frac{\pi}{4}\right)$
$Bi(-u) \to \frac{1}{\sqrt{\pi}u^{1/4}}\cos\left(\zeta+\frac{\pi}{4}\right)$,	$Bi'(-u) \to \frac{1}{\sqrt{\pi}}u^{1/4}\sin\left(\zeta+\frac{\pi}{4}\right)$.

Source: Data from M. Abramowitz and I. A. Stegun, eds., *Handbook of Mathematical Functions*, National Bureau of Standards, Washington, D.C., 1964.

[a] $\zeta = \frac{2}{3}u^{3/2}$.

The wavefunction given by Eq. (W19B.9) and its first derivative at $z = 0$ are set equal to the corresponding quantities given by Eq. (W19B.5). Solving these equations for N yields

$$N = \frac{2ik_z\sqrt{\pi}\ e^{-\zeta_0}L^{-3/2}}{ik_z/u_0^{1/4} - Fu_0^{1/4}(2m/\hbar^2F^2)^{1/3}}, \tag{W19B.11}$$

where $u_0 = (2m/\hbar^2F^2)^{1/3}(V_0 - \hbar^2k_z^2/2m)$, $\zeta_0 = \frac{2}{3}u_0^{3/2}$, and L^3 is the volume of the metal.

The current density is obtained by integrating Eq. (19B.10) over the Fermi sphere:

$$J = \sum_s \sum_{\mathbf{k}} J_z\Theta(E_F - E) = 2\int \frac{d^3kL^3}{(2\pi)^3}J_z\Theta(E_F - E). \tag{W19B.12}$$

The integration over transverse coordinates leads to

$$\int d^2k_\parallel\Theta(E_F - E) = \pi\left(\frac{2mE_F}{\hbar^2} - k_z^2\right)\Theta\left(\frac{2mE_F}{\hbar^2} - k_z^2\right). \tag{W19B.13}$$

Thus one obtains

$$J = \frac{2me}{\pi^2\hbar^3V_0}\int_0^{E_F} dE'(E_F - E')\sqrt{E'(V_0 - E')}\exp\left[-\frac{4\sqrt{2m}}{3F\hbar}(V_0 - E')^{3/2}\right]. \tag{W19B.14}$$

The major contribution to the integral comes from the region $E' = E_F$. Thus one may make the replacements $(V_0 - E')^{3/2} \approx W^{3/2} + \frac{3}{2}\sqrt{W}(E_F - E')$, $E'(V_0 - E') \approx E_FW$ and extend the lower limit of the integral to $-\infty$. Here W is the work function. One finally obtains the Fowler–Nordheim formula:

$$J = \frac{e^3E_0^2}{4\pi^2\hbar V_0}\sqrt{\frac{E_F}{W}}\exp\left(-\frac{4}{3eE_0\hbar}\sqrt{2mW^3}\right). \tag{W19B.15}$$

An additional correction may be included to account for the image potential that the charge experiences when it is in the vacuum region, but it will not be included here.

Appendix W19C: Photoemission Yields

In this appendix theoretical expressions for the photoelectric yield will be derived for an idealized solid whose surface consists of a potential step. The Sommerfeld model will be used to describe the electrons.

First, the simplifying assumption that the potential is only a function of the normal coordinate, z, will be made. The wavefunctions are then of the form

$$\psi_f(\mathbf{r}) = \phi_f(z)\exp(i\mathbf{k}'_\parallel \cdot \mathbf{r}_\parallel), \tag{W19C.1a}$$

$$\psi_i(\mathbf{r}) = \phi_i(z)\exp(i\mathbf{k}_\parallel \cdot \mathbf{r}_\parallel), \tag{W19C.1b}$$

where the subscripts f and i refer to the final and initial states, respectively, and $\mathbf{k}_\parallel$ and $\mathbf{k}'_\parallel$ refer to propagation vectors along the surface.

Write the matrix element in Eq. (19.29) as

$$\langle\psi_f|\boldsymbol{\mu}\cdot\mathbf{E}|\psi_i\rangle = -e\langle\psi_f|\mathbf{r}_\parallel\cdot\mathbf{E}_\parallel|\psi_i\rangle - e\langle\psi_f|zE_z|\psi_i\rangle. \tag{W19C.2}$$

By introducing the Hamiltonian, H, the first term can be shown to vanish:

$$\begin{aligned}\langle\psi_f|\mathbf{r}_\parallel\cdot\mathbf{E}_\parallel|\psi_i\rangle &= \frac{1}{E_f - E_i}\langle\psi_f|[H, \mathbf{r}_\parallel\cdot\mathbf{E}_\parallel]|\psi_i\rangle \\ &= -\frac{i}{m\omega}\langle\psi_f|\mathbf{p}_\parallel\cdot\mathbf{E}_\parallel|\psi_i\rangle = -\frac{i\hbar}{m\omega}\mathbf{k}_\parallel\cdot\mathbf{E}_\parallel\langle\psi_f|\psi_i\rangle = 0.\end{aligned} \tag{W19C.3}$$

In this model it is only the normal component of the electric field that is capable of exciting the electron gas and of causing photoemission. Any photoemission observed at normal incidence, in which case the electric field would be tangent to the surface, would be considered volume photoemission and beyond the scope of the model.

The full Hamiltonian governing the interaction of the electron with the light is

$$H = H_0 + H_\gamma = \frac{p^2}{2m} + V(z) + eE_z z[\exp(\lambda z)\Theta(-z) + \Theta(z)] + e\mathbf{E}_\parallel\cdot\mathbf{r}_\parallel. \tag{W19C.4}$$

The last term is the interaction of the electron with the component of the field parallel to the surface, and can be dropped. The third term is the perturbation, H_γ. For the initial state the unperturbed Schrödinger equation becomes

$$\left[\frac{p_z^2}{2m} + V(z) - \varepsilon_i\right]\phi_i(z) = 0, \tag{W19C.5a}$$

and for the final state,

$$\left[\frac{p_z^2}{2m} + V(z) - \varepsilon_f\right]\phi_f(z) = 0, \tag{W19C.5b}$$

where

$$\varepsilon_i = E_i - \frac{\hbar^2 k_\parallel^2}{2m}, \tag{W19C.6a}$$

$$\varepsilon_f = E_f - \frac{\hbar^2 k_\parallel^2}{2m}. \tag{W19C.6b}$$

The Schrödinger equation will be solved for the simple step potential:

$$V(z) = \begin{cases} 0 & \text{if} \quad z > 0 \\ -V_0 & \text{if} \quad z < 0. \end{cases} \tag{W19C.7}$$

(The effect of a finite electron mean free path could, in principle, be included by making V_0 complex.)

For the initial state the solution was found in Eq. (19.8) in the discussion of relaxation of metals. Thus

$$\phi_i(z) = \begin{cases} B\exp(-\kappa z) & \text{if} \quad z > 0 \\ \dfrac{B\sin(qz+\delta)}{\sin\delta} & \text{if} \quad z < 0 \end{cases} \tag{W19C.8}$$

where

$$\kappa = \frac{1}{\hbar}\sqrt{-2m\varepsilon_i}, \tag{W19C.9a}$$

$$q = \frac{1}{\hbar}\sqrt{2m(V_0+\varepsilon_i)}. \tag{W19C.9b}$$

For the final state one has an *out-state*, an outgoing wave with unit amplitude in the vacuum supplemented with incoming waves in both the vacuum and the metal. (A packet constructed out of such states will evolve into a purely outgoing packet for long times.) Thus

$$\phi_f = \begin{cases} \exp(ikz) + r\exp(-ikz) & \text{if} \quad z > 0, \\ t\exp(iq'z) & \text{if} \quad z < 0, \end{cases} \tag{W19C.10}$$

where

$$k = \frac{1}{\hbar}\sqrt{2m\varepsilon_f}, \tag{W19C.11a}$$

$$q' = \frac{1}{\hbar}\sqrt{2m(\varepsilon_f + V_0)} \tag{W19C.11b}$$

Matching the wavefunction and the derivative at $z = 0$ yields

$$t = 1 + r, \tag{W19C.12a}$$

$$q't = k(1 - r). \tag{W19C.12b}$$

Then the reflection amplitude is

$$r = \frac{k - q'}{k + q'}, \tag{W19C.13a}$$

and the transmission amplitude is

$$t = \frac{2k}{k + q'}. \tag{W19C.13b}$$

The matrix element of the perturbation is

$$\langle \psi_f | H_\gamma | \psi_i \rangle = \int d^2 r_\parallel \exp\lceil i(\mathbf{k}_\parallel - \mathbf{k}'_\parallel) \cdot \mathbf{r}_\parallel \rceil \times eE_z \int_{-\infty}^{\infty} dz\, \phi_f^*(z) z [\exp(\lambda z)\Theta(-z) + \Theta(z)]\phi_i(z), \tag{W19C.14}$$

which may be written as

$$\langle \psi_f | H_\gamma | \psi_i \rangle = eE_z (2\pi)^2 \delta(\mathbf{k}'_\parallel - \mathbf{k}_\parallel)(I_1 + I_2). \tag{W19C.15}$$

The first integral is

$$I_1 = \frac{t^* B}{\sin\delta} \int_{-\infty}^{0} dz z\ \exp[z(\lambda - iq')] \sin(qz + \delta) - \frac{t^* B}{2i \sin\delta} \left[\frac{\exp(i\delta)}{[\lambda + i(q - q')]^2} - \frac{\exp(-i\delta)}{[\lambda - i(q + q')]^2} \right], \tag{W19C.16a}$$

and the second integral is

$$I_2 = \int_0^\infty [\exp(-ikz) + r^* \exp(ikz)] z B\ \exp(-\kappa z) dz = B \left[\frac{1}{(\kappa + ik)^2} + \frac{r^*}{(\kappa - ik)^2} \right]. \tag{W19C.16b}$$

Plugging this into Fermi's golden rule gives the transition rate per unit area:

$$\frac{d\Gamma}{dA} = \frac{2\pi}{\hbar} \sum_s \int \frac{d^2 k_\parallel}{(2\pi)^2} \int_0^\infty \frac{dq}{\pi} \int \frac{d^2 k'_\parallel}{(2\pi)^2} \int_{-\infty}^{\infty} \frac{dk}{2\pi} 2\ \sin^2\delta (eE_z)^2 (2\pi)^2 \delta(\mathbf{k}'_\parallel - \mathbf{k}_\parallel) |M|^2 \times \delta(E_i + \hbar\omega - E_f)\Theta(k)\Theta(E_F - E_i)\Theta(E_f - E_F). \tag{W19C.17}$$

where E_F is the Fermi energy level and

$$M = -\frac{t^* \exp(i\delta)}{2i \sin\delta [\lambda + i(q - q')]^2} + \frac{t^* \exp(-i\delta)}{2i \sin\delta [\lambda - i(q + q')]^2} + \frac{1}{(\kappa + ik)^2} + \frac{r^*}{(\kappa - ik)^2}. \tag{W19C.18}$$

The photoelectric yield is obtained by dividing this by the incident number of photons per unit area:

$$Y = \frac{d\Gamma / dA}{I / \hbar\omega} = \frac{8\pi\hbar\omega}{cE_0^2} \frac{d\Gamma}{dA}. \tag{W19C.19}$$

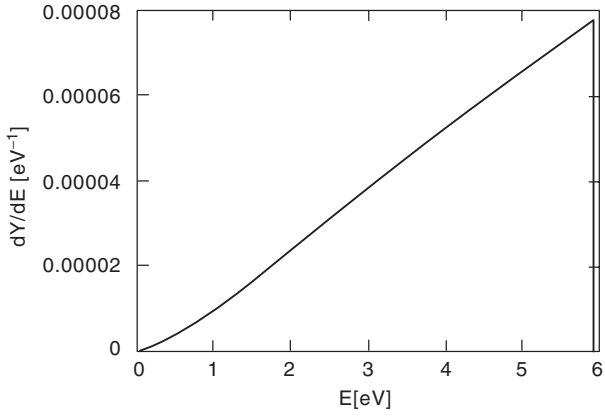

Figure W19C.1. Theoretical differential photoelectric yield of emitted electrons for Al irradiated with 10.2-eV photons. The quantity $dY/d\varepsilon_F$ is defined in Eq. (W19C.22).

The transverse wave-vector integral is

$$\int \frac{d\mathbf{k}_\parallel}{(2\pi)^2}\Theta\left(E_F-\varepsilon_i-\frac{\hbar^2k_\parallel^2}{2m}\right)\Theta\left(-E_F+\varepsilon_f+\frac{\hbar^2k_\parallel^2}{2m}\right)$$
$$=\frac{m}{2\pi\hbar^2}[E_F-\varepsilon_i-\max(0,E_F-\varepsilon_f)]\Theta(E_F-\varepsilon_i-\max(0,E_F-\varepsilon_f)). \quad \text{(W19C.20)}$$

After evaluating the remaining integrals, one finds that

$$Y=\frac{16m\omega e^2}{\pi\hbar^2c}\sin^2\theta\int_0^\infty dq\int_0^\infty dk|M|^2\sin^2\delta\;\delta(\varepsilon_f-\varepsilon_i-\hbar\omega)$$
$$\times\,[E_F-\varepsilon_i-\max(0,E_F-\varepsilon_f)]\Theta(E_F-\varepsilon_i-\max(0,E_F-\varepsilon_f)), \quad \text{(W19C.21)}$$

where θ is the angle of incidence relative to the surface normal.

The *energy distribution curve* (EDC) is obtained by omitting the integration over the variable k and using the energy-conserving delta function to do the q integration. The result is expressed in terms of ε_f:

$$\frac{dY}{d\varepsilon_f}=\frac{8}{\pi}\frac{m^2e^2\omega}{\hbar^4C}\sin^2\theta\frac{|M^2|\sin^2\delta}{\sqrt{\varepsilon_f(V_0+\varepsilon_f-\hbar\omega)}}[E_F-\varepsilon_f+\hbar\omega-\max(0,E_F-\varepsilon_f)]$$
$$\times\,\Theta[E_F-\varepsilon_f+\hbar\omega-\max(0,E_F-\varepsilon_f)]\Theta(\varepsilon_f+V_0-\hbar\omega). \quad \text{(W19C.22)}$$

It is straightforward to show that near threshold the matrix element M is proportional to k.

A theoretical electron EDC is presented for Al in Fig. W19C.1. This is to be compared with experimental results, as shown in Fig. 19.13. In both cases one notes a rise in the photoyield with increasing energy followed by a precipitous drop at high energy, corresponding to electrons emerging from the Fermi surface, giving rise to those with maximum kinetic energy, $(mv^2/2)_{\max}$. There is evidence for band-structure features in the experimental data. Band-structure effects are not included in the simple Sommerfeld model used here.